



University
of Glasgow

Small, D., Austin, W., and Rinterknecht, V. (2013) Freshwater influx, hydrographic reorganisation and the dispersal of ice rafted detritus in the sub-polar North Atlantic Ocean during the last deglaciation. *Journal of Quaternary Science*, 28 (5). pp. 527-535. ISSN 0267-8179

Copyright © 2013 John Wiley & Sons, Ltd.

A copy can be downloaded for personal non-commercial research or study, without prior permission or charge

Content must not be changed in any way or reproduced in any format or medium without the formal permission of the copyright holder(s)

When referring to this work, full bibliographic details must be given

<http://eprints.gla.ac.uk/86502>

Deposited on: 22 October 2013



Freshwater influx, hydrographic reorganization and the dispersal of Ice Rafted Detritus in the sub-polar North Atlantic Ocean during the last deglaciation.

Journal:	<i>Journal of Quaternary Science</i>
Manuscript ID:	JQS-13-0031.R1
Wiley - Manuscript type:	Research Article
Date Submitted by the Author:	n/a
Complete List of Authors:	Small, David; University of Glasgow, Department of Geographical and Earth Sciences Austin, William; University of St Andrews, Geography and Geosciences Rinterknecht, Vincent; University of St Andrews, Geography and Geosciences; University of St. Andrews , Geography and Geosciences;
Keywords:	Ice rafted detritus, North Atlantic, deglaciation, hydrography, Sea surface temperature

SCHOLARONE™
Manuscripts

1
2
3 1 Freshwater influx, hydrographic reorganisation and the dispersal of Ice
4
5
6 2 Rafted Detritus in the sub-polar North Atlantic Ocean during the last
7
8
9 3 deglaciation.

10
11
12 4 David Small^{1*}, William Austin¹, Vincent Rinterknecht¹

13
14 5 School of Geography and Geosciences, University of St Andrews, St Andrews, Scotland.

15
16 6 *Now at School of Geographical and Earth Sciences, University of Glasgow, Glasgow,
17 7 Scotland.

18
19 8

20
21 9 Corresponding author D. Small, School of Geographical and Earth Sciences University of
22 10 Glasgow, Glasgow, Scotland G12 8QQ. Email: David.Small@glasgow.ac.uk

23
24 11

25
26 12 **ABSTRACT**

27
28 13 A sediment core from the northeast North Atlantic contains high-resolution co-registered
29
30 14 foraminiferal $\delta^{18}\text{O}$ and IRD record for the last deglaciation. These reveal a distinct ice-rafting
31
32 15 event that occurred at the time of Greenland Interstade 1d (GI-1d), a feature also seen in other
33
34 16 high-resolution cores from the North Atlantic. The occurrence of a geographically widespread
35
36 17 peak in ice rafted detritus (IRD) at ice distal sites at a time when increased freshwater flux to
37
38 18 the surface ocean is inferred to have caused rapid cooling suggests a mechanistic link between
39
40 19 the processes, analogous to the Younger Dryas (GS-1) cooling episode. The general absence
41
42 20 of IRD at southern locations at other times during GI-1 when the flux of icebergs from
43
44 21 surviving ice sheets to northern locations continued, suggests that the GI-1d IRD peak
45
46 22 represents a time of hydrographic reorganisation which changed IRD dispersal. While
47
48 23 numerous studies have suggested freshwater flux as a major driver of rapid climate
49
50 24 oscillations observed around the North Atlantic during the last deglaciation, the evidence
51
52 25 presented here both supports that mechanism and highlights the potential for rapid and major
53
54
55
56
57
58
59
60

1
2
3 26 reorganisation of the of the North Atlantic's surface hydrography to explain changes in IRD
4
5 27 flux independently of ice sheet calving dynamics.
6
7

8 28
9

10 29 **Key Words**

11 30 Ice rafted detritus, North Atlantic, deglaciation, sea surface temperature, hydrography.
12
13

14 31
15
16
17
18
19
20
21
22
23
24
25
26
27
28
29
30
31
32
33
34
35
36
37
38
39
40
41
42
43
44
45
46
47
48
49
50
51
52
53
54
55
56
57
58
59
60

1. Introduction

High-resolution records spanning the Last Glacial-Interglacial Transition (LGIT) have consistently revealed a climate system punctuated by numerous abrupt climate transitions (Severinghaus and Brook, 1999; Alley *et al.*, 2003; Steffensen *et al.*, 2008). Several of these events have been linked to changes in Atlantic Meridional Overturning Circulation (AMOC) and its associated heat flux because of its sensitivity to increased freshwater input (Clark *et al.*, 2001; Clark *et al.*, 2002a; McManus *et al.*, 2004). To firmly establish freshwater forcing as an underlying causal mechanism of these abrupt climate transitions requires firstly, well constrained chronostratigraphies such that events can be correlated between records with confidence and, secondly, widespread geological evidence that links the North Atlantic's surface conditions to changes in the deep and intermediate ocean.

The occurrence of Ice Rafted Detritus (IRD) within marine sediments has long been used to investigate the links between climate, oceans and ice sheets (Heinrich, 1988; Bond *et al.*, 1993; Elliot *et al.*, 2001; Knutz *et al.*, 2001; Hemming, 2004; Peck *et al.*, 2007; Hendy and Cosma, 2008; Scourse *et al.*, 2009). In order to fully understand these links, it is not only important to understand how variations in IRD relate to ice sheet advance and/or retreat (McCabe and Clark, 1998; Marshall and Koutnik, 2006) but also to develop an understanding of the way hydrographic controls can influence the dispersal of IRD within an oceanic basin. There has been relatively little work relating hydrographic factors to IRD records, although some authors have argued for minimal hydrographic control in parts of the sub-polar North Atlantic (Elliot *et al.*, 2001) and in relation to the first occurrences of Heinrich like events in the earlier Pleistocene (Naafs *et al.*, 2011). One situation where hydrographic controls have been cited as influencing the pattern of IRD deposition is in regards to the location of the IRD Belt (Figure 1) (Ruddiman, 1977; Ruddiman and McIntyre, 1981; Scourse *et al.*, 2009).

1
2
3 56 Potential hydrographic controls include the pattern of oceanic surface currents which
4
5 57 affect the dispersal of icebergs and thus IRD and, potentially more importantly, sea surface
6
7 58 temperature (SST). Palaeoclimatic records indicate that large and abrupt changes to AMOC
8
9 59 during the last glacial period were associated with changes in climate (Vidal *et al.*, 1997;
10
11 60 Austin and Kroon, 2001; Clark *et al.*, 2002a; Rahmstorf, 2002; McManus *et al.*, 2004;
12
13 61 Thornalley *et al.*, 2010). Freshwater input to the North Atlantic is suggested to be one of the
14
15 62 major drivers of changes to AMOC and attendant climatic impacts (Broecker, 1994). This
16
17 63 link is supported by proxy data (Elliot *et al.*, 2002; McManus *et al.*, 2004) and modeling
18
19 64 studies (LeGrande *et al.*, 2006; Clarke *et al.*, 2009; Liu *et al.*, 2009; He *et al.*, 2013), which
20
21 65 demonstrate that a weakening of AMOC is associated with cooling and lower SSTs. SSTs
22
23 66 influence the melt rates of icebergs and hence their longevity in the open ocean; as such,
24
25 67 icebergs are more likely to travel large distances across ocean basins during times of lower
26
27 68 SSTs. IRD peaks in ice distal sites at these times may reflect the increased persistence and
28
29 69 dispersal of icebergs, relating to hydrographic conditions, rather than an increased total flux of
30
31 70 icebergs related to ice sheet dynamics. Comparing IRD records from distal sites with records
32
33 71 relating to temporal variations in iceberg flux (both proximal and distal) can allow these links
34
35 72 to be investigated.

36
37
38
39
40
41 73 High resolution records spanning the LGIT are punctuated by numerous IRD events
42
43 74 which some authors have linked directly to changes in ice sheet dynamics (eg: Knutz *et al.*,
44
45 75 2001), given the potential influence of SST variations highlighted above it is imperative to
46
47 76 establish if making such inferences is valid. Such an understanding will aid attempts to
48
49 77 integrate records of oceanic changes with ice sheet behaviour and explore the two-way forcing
50
51 78 relationship that exists (Clark *et al.*, 2001). Here we present a new, high resolution IRD record
52
53 79 from the northeast North Atlantic and use it to identify a distinct and widespread LGIT ice
54
55 80 rafting event. It's timing, as indicated by a major change in the co-registered foraminiferal
56
57
58
59
60

1
2
3 81 $\delta^{18}\text{O}$, coincides with the cold interval of GI-1d (Lowe *et al.*, 2008). Episodic freshwater input
4
5 82 to the North Atlantic has been proposed as the cause of such cold intervals that punctuate the
6
7 83 LGIT (Thornalley *et al.*, 2010). Establishing the effects of such input has important
8
9
10 84 implications for our understanding of rapid climate change during the last deglaciation as it
11
12 85 provides a linking mechanism between ice sheets and changes in oceanic circulation.
13
14
15 86

18 87 **2. Study site and methods.**

20 88

22 89 **2.1. Study site**

24 90 Giant Piston Core MD95-2007 was collected in 1995 from the *RV Marion Dufresne* in
25
26 91 the St Kilda basin on the Hebridean shelf, Northwest Scotland (57° 31.057' N, 08° 23.171' W,
27
28 92 158 m water depth, 19.35m recovery; Figure 1). The St Kilda basin is a glacially over-
29
30
31 93 deepened basin that is within the limits of the last British-Irish Ice Sheet (BIIS) (Davies *et al.*,
32
33 94 1984; Peacock *et al.*, 1992; Stoker *et al.*, 1993). This conclusion is supported by a ^{14}C date of
34
35 95 22,480±300 ^{14}C a BP (27.1 cal ka BP [OxCal v4.1 (Bronk-Ramsey, 2009), MARINE09
36
37 96 (Reimer *et al.*, 2009)]) on marine shell material to the west of morainal banks marking the
38
39
40 97 aforementioned BIIS limit and of 'basal' ages <16 ^{14}C ka BP (<19 cal ka BP) within those
41
42 98 same limits (Peacock *et al.*, 1992; Austin and Kroon, 1996). These ages demonstrate that this
43
44 99 sector of the BIIS was at its maximum extent prior to 20 ka. As MD95-2007 is located within
45
46 100 these ice limits it is thought to record nearly the entire deglacial sequence following initial
47
48
49 101 deglaciation of the shelf edge.

51
52 102 The potential for cores recovered from the St Kilda basin to record high-resolution
53
54 103 records of the LGIT was initially demonstrated from two vibrocores VE57/-09/89 and VE57/-
55
56 104 09/46 (Austin, 1991; Peacock *et al.*, 1992; Austin and Kroon, 1996). These cores showed an
57
58
59
60

1
2
3 105 expanded LGIT sedimentary sequence but a poorly resolved Holocene sequence. From the
4
5 106 variety of sedimentary, micropalaeontological and isotopic evidence recorded in these cores it
6
7 107 was proposed that the St Kilda basin deglaciated at 15.2 ^{14}C ka BP (17.6 cal ka BP) after
8
9 108 which its waters remained cold with low salinity until 13.5 ^{14}C ka BP (15.6 cal ka BP).
10
11 109 Following this time, mostly warm interstadial conditions prevailed until a major cooling
12
13 110 associated with the onset of GS-1 was observed at 11.6 ^{14}C ka BP (13.0 cal ka BP). The
14
15 111 return to warm temperatures at the beginning of the Holocene occurred prior to 10 ^{14}C ka BP
16
17 112 (11 cal ka BP) (Austin and Kroon, 1996).
18
19
20
21
22
23

113

24 114 **2.2. A revised chronostratigraphy for MD95-2007**

25
26 115 The original age model for MD95-2007 (Wilson, 2004) was based on 16 AMS ^{14}C
27
28 116 ages calibrated using Calib4_2 (Stuiver and Reimer, 1993; Stuiver *et al.*, 1998), following a
29
30 117 reservoir correction ($R_{(t)}$) reflecting the modern values of seawater (i.e. $\Delta R=0$). The
31
32 118 availability of a $\delta^{18}\text{O}$ record ($\delta^{18}\text{O}_{\text{foram}}$), measured in the epi-benthic foraminifera *Cibicides*
33
34 119 *lobatulus* (originally reported in Austin *et al.*, 2011), provides an additional means of
35
36 120 improving the age-depth relationship. Given the rapid and abrupt nature of the GI-1 climate
37
38 121 oscillations, the high resolution of the MD95-2007 $\delta^{18}\text{O}_{\text{foram}}$ record and inherent uncertainty
39
40 122 about the variable marine reservoir effect during this period (Austin *et al.*, 1995; 2011), it is
41
42 123 important to determine the timing of particular climatic episodes during GI-1 *vis à vis* the
43
44 124 candidate cold episodes GI-1d or GI-1b (Figure 3). This is done by constraining the $\delta^{18}\text{O}_{\text{foram}}$
45
46 125 record using recalibrated AMC ^{14}C ages (OxCal v4.1, MARINE09 (Bronk-Ramsey, 2009;
47
48 126 Reimer *et al.*, 2009) with three different values for $R_{(t)}$: the modern value 400 years ($\Delta R = 0$),
49
50 127 the commonly cited GS-1 value 700 years ($\Delta R = 300$) and a maximum value of 1,100 years
51
52 128 ($\Delta R = 700$) (Waelbroeck *et al.*, 2001). This approach provides a good first order constraint to
53
54
55
56
57
58
59
60

1
2
3 129 the age of the interstadial $\delta^{18}\text{O}_{\text{foram}}$ excursion (Austin *et al.*, 2011). In order for this excursion
4
5 130 to correlate with GI-1b (13.3-13.1 ka b2k) the reservoir age correction would need to exceed
6
7 131 1000 years (Figure 3). A reconstruction of $R_{(t)}$ at this time from MD95-2007 indicates that it
8
9
10 132 was lower than the GS-1 value of ~ 1000 years (Austin *et al.*, 2011) thus the $\delta^{18}\text{O}_{\text{foram}}$
11
12 133 excursion is correlated with GI-1d (Figure 3).

13
14
15 134 Based upon this interpretation of the climate event-stratigraphy, the $\delta^{18}\text{O}_{\text{foram}}$
16
17 135 stratigraphy can be tuned to the NGRIP $\delta^{18}\text{O}_{\text{ice}}$ record using the GICC05 chronology
18
19
20 136 (Rasmussen *et al.*, 2006). For the rapid $\delta^{18}\text{O}_{\text{foram}}$ changes at the onset and end of GS-1 and
21
22 137 GI-1d the tie-point was assigned to the mid-point of the transition. The Vedde Ash has been
23
24 138 indentified within MD95-2007 and more widely across the St Kilda basin (Austin *et al.*, 1995;
25
26 139 Peters *et al.*, 2010; Austin *et al.*, 2011). This tephra occurs at a core depth of 281 cm and has
27
28
29 140 been assigned an age of 12,171 a b2k (Rasmussen *et al.*, 2006). Table 2 summarizes the tie-
30
31 141 points, their core depths and the ages assigned to them. During this interval the age
32
33 142 uncertainty within the GICC05 timescale is 100-200 years (Rasmussen *et al.*, 2006) however
34
35 143 as we are comparing tuned records this has no influence on our conclusions. This age model
36
37 144 follows the INTIMATE protocols (Lowe *et al.*, 2008; Austin and Hibbert, 2012). It must be
38
39 145 noted that this approach assumes synchronicity and therefore any information about time
40
41
42 146 leads/lags is lost and conclusions based on the results must respect this limitation.

43
44
45 147 One complicating factor in the use of the tuning method to construct an age model for
46
47 148 MD95-2007 is that there is no obvious structure to the local climate event-stratigraphy beyond
48
49 149 the cold excursion GI-1d. As a result age control in the lower section of the core is difficult,
50
51
52 150 further dating may improve this but would be hampered by a general scarcity of suitable
53
54 151 material in the lower core (Austin pers. Comm). To anchor the base of the record it is
55
56 152 therefore necessary to use the basal radiocarbon determination ($13,950 \pm 130$ ^{14}C a BP) at a
57
58
59
60

1
2
3 153 depth of 1821 cm. This subsequently introduces an uncertainty related to the choice of $R_{(t)}$
4
5 154 used in the correction and then calibration of this age. The differences in the basal age
6
7 155 calculated using the various corrections are significant and would affect any interpretations
8
9
10 156 based on the timing of events in the lower 0.6 m of our record. For this reason we avoid
11
12 157 making interpretations based on data from the un-tuned section of the age model which must
13
14 158 be considered tentative. The effects of a variable correction are, however, restricted to this
15
16 159 basal section of the core and are not a key factor when considering the tuned section to which
17
18 160 this study relates.
19

20
21
22 161

23 24 162 **2.3. A new IRD record from MD95-2007**

25
26 163 IRD_{flux} is calculated from the IRD concentration and bulk mass accumulation rate
27
28 164 (BMAR), such that:

$$29
30
31 165 \quad IRD_{flux} = IRD_{conc} * BMAR$$

32
33
34
35 166 The BMAR in turn is calculated using a linear sedimentation rate (LSR) derived from the age
36
37 167 model and the dry bulk density (ρ_{DB}) of the sediment such that:

$$38
39
40 168 \quad BMAR = LSR * \rho_{DB}$$

41
42
43 169 Calculation of the LSR involves linear interpolation between the tie points used in
44
45 170 construction of the core's age model. ρ_{DB} is calculated using the wet and dry mass of known
46
47 171 volumes of sediment assuming sediment particle and pore water densities of 2650 and 1025 kg
48
49 172 m^{-3} and pore water salinity of 35 $g\ kg^{-1}$.

50
51
52
53 173 Lithic counts were carried out on the coarse (>250 μm) fraction. Traditionally, grains
54
55 174 coarser than 150 μm are considered to be ice rafted (Hemming, 2004), but we use a coarser
56
57
58
59
60

175 fraction because of the possibility that the shelf was a higher energy environment compared to
176 the deep ocean, especially at times, such as the LGIT, when sea level was lower.

177

178 3. Results

179 The IRD_{flux} record from core MD95-2007, plotted against the benthic $\delta^{18}\text{O}_{\text{foram}}$ record
180 (Figure 4), shows 3 periods of increased IRD flux to the core site. The initial, and highest,
181 period of increased flux occurs near the base of the core. IRD_{flux} during this time consistently
182 exceeds 150,000 grains $\text{cm}^{-2} \text{a}^{-1}$. This period corresponds to the missing part of the $\delta^{18}\text{O}_{\text{foram}}$
183 stratigraphy such that age-control is poor and resultant IRD flux uncertainty relatively high.
184 Following this there is a period of near zero IRD_{flux} which lasted until ~ 14.1 ka. The
185 subsequent peak in IRD corresponds to a significant $\delta^{18}\text{O}_{\text{foram}}$ excursion correlated to GI-1d
186 (see section 2.2). After this brief (121 ± 4 a; NGRIP/GICC05 timescale) period IRD_{flux} returns
187 to the very low background levels observed prior to GI-1d. This low rate continues until a
188 slow increase in IRD_{flux} prior to the onset of GS-1 that is marked by a distinct increase in the
189 IRD_{flux} to the core site. Following the end of GS-1, as defined in the $\delta^{18}\text{O}_{\text{foram}}$ stratigraphy,
190 IRD_{flux} rates are zero.

191

192 4. Discussion

193 The period of increased IRD_{flux} centered on 14.1 ka coincides with a $\delta^{18}\text{O}_{\text{foram}}$
194 excursion that has been correlated with the cold oscillation GI-1d observed within the NGRIP
195 $\delta^{18}\text{O}_{\text{ice}}$ record (Rasmussen *et al.*, 2006). Recent provenance work using U-Pb dating of detrital
196 minerals identifies a distinct distal component to the IRD found within MD95-2007, inferred
197 to be sourced from north eastern Canada, Baffin Island or East Greenland (Small *et al.*, 2013).
198 The provenance data presented by Small *et al.* (2013) do not preclude a contribution from

1
2
3 199 local sources (i.e. the BIIS) and the abundance of coarse ($>250\ \mu\text{m}$) is suggestive of a local
4
5 200 source given the relationship between IRD grain size and transport distance (Andrews, 2000).
6
7 201 However, it is doubtful that the BIIS had marine margins capable of supplying IRD to the
8
9 202 offshore environment at this time (Bradwell *et al.*, 2008; Ballantyne and Stone, 2012). It is
10
11 203 possible that grain-specific provenance studies may be biased particularly if the analysed
12
13 204 grains come from a particular size fraction. Despite this potential limitation the distinct distal
14
15 205 signal identified within the IRD provenance data provides clear evidence that IRD was
16
17 206 transported some distance across the North Atlantic during the short cold oscillation GI-1d.
18
19

20
21 207 The IRD_{flux} and benthic $\delta^{18}\text{O}_{\text{foram}}$ records from MD95-2007 are shown in comparison
22
23 208 to proxy records from several other North Atlantic cores (DAPC-2, RAPid-15-4P, TTR-451;
24
25 209 Figure 5). The highlighted peak in IRD_{flux} observed at 14.1 ka, which is co-registered with a
26
27 210 $\delta^{18}\text{O}_{\text{foram}}$ excursion within MD95-2007, also coincides with distinct increases in the IRD
28
29 211 records in both DAPC-2 and RAPid-15-4P indicating some common mechanism is
30
31 212 responsible. However, it should be pointed out that the IRD record from RAPid-15-4P is
32
33 213 concentration rather than flux however the consistent pattern between this and the flux records
34
35 214 (MD-95-2007, DAPC-2) gives us confidence that it records the same event.
36
37
38
39

40 215 The IRD peak in RAPid-15-4P corresponds to the occurrence of an Icelandic tephra
41
42 216 interpreted as being the Katla Ash. This tephra is also observed within the NGRIP record and
43
44 217 can thus be assigned a precise age of 14.02 ka b2k (Thornalley *et al.*, 2010; Rasmussen *et al.*,
45
46 218 2006). The age model of DAPC-2 was constructed by visual tuning of the Nps% record with
47
48 219 the GISP2 $\delta^{18}\text{O}$ record (Knutz *et al.*, 2007) which results in an age offset compared to the
49
50 220 cores tuned to the NGRIP record (Figure 10 in Rasmussen *et al.*, 2006). The availability of
51
52 221 AMS radiocarbon dates within this core is not sufficient to independently verify the tuning in
53
54 222 this part of the stratigraphy. However, the stratigraphic position of the IRD peak suggests that
55
56
57
58
59
60

1
2
3 223 it is correlative to GI-1d as it occurs at the same time as the earliest recorded peak in Nps%
4
5 224 during GI-1. This strongly indicates that the IRD peak represents the same event that is seen
6
7 225 in MD95-2007 and RAPid-15-4P.
8
9

10 226 Considering the evidence for a distal contribution of IRD during GI-1d (Small *et al.*,
11 227 2013) it can be hypothesised that, *if* the overall flux of icebergs to the North Atlantic from
12 228 these distal sources is the fundamental control on the occurrence of IRD within MD95-2007,
13 229 then the MD95-2007 IRD_{flux} record should reflect variations in this flux. A similar
14 230 relationship should exist during GI-1 for DAPC-2, which is inferred to have been
15 231 predominantly supplied with BIIS sourced IRD for most of its history (Knutz *et al.*, 2007).
16 232 Obtaining comparable provenance data from DAPC-2 would allow this assumption to be
17 233 tested.
18
19
20
21
22
23
24
25
26
27
28

29 234 The IRD peaks during GI-1 seen within DAPC-2 and RAPid-15-4P occur during times
30 235 of low SST indicated by relative high abundance of the planktonic foraminifera *N.*
31 236 *pachyderma* sinistral (Nps%) (Knutz *et al.*, 2007; Thornalley *et al.*, 2010). The correlation
32 237 between IRD peaks and peaks in Nps% indicates that they occurred during times when the
33 238 sites were located north of the Polar Front (Scourse *et al.*, 2009). If the observed GI-1d IRD
34 239 peaks simply reflected an increased flux of IRD to the North Atlantic, then it would be
35 240 expected that they would record IRD at other times when it is recorded in ice proximal core
36 241 sites. Core TTR-451 from the Eirik Drift (Stanford *et al.*, 2011) shows increased IRD flux
37 242 throughout GI-1. It can be inferred from this that significant amounts of icebergs were calved
38 243 from the Greenland Ice Sheet (GIS) at times when no IRD was reaching the distal core sites.
39 244 Furthermore, models suggest that the GIS would have maintained calving margins for a large
40 245 part of GI-1, providing a persistent possible source for icebergs (Simpson *et al.*, 2009). This
41 246 implies that some other control was acting to prevent deposition at the ice distal sites at times
42 247 of continuing iceberg flux to higher latitudes.
43
44
45
46
47
48
49
50
51
52
53
54
55
56
57
58
59
60

1
2
3 248 A series of rapid variations in SST are observed in the Nps% records from cores
4
5 249 DAPC2 and RAPid-15-4P (Knutz *et al.*, 2007; Thornalley *et al.*, 2010). In each core one of
6
7 250 these variations is correlated with GI-1d and is coincident with the GI-1 IRD peak. Nps%
8
9
10 251 peaks indicating cooler periods of SST during GI-1 are also seen in core MD95-2006, taken
11
12 252 from the Barra fan, <100 km south west of MD95-2007 (Wilson *et al.*, 2002; Peters *et al.*,
13
14 253 2010; Hibbert *et al.*, 2010). It is reasonable to assume that one of the peaks corresponds to
15
16 254 GI-1d given the widespread and simultaneous nature of climate change in the North Atlantic
17
18 255 at this time (Bjorck *et al.*, 1996; Broecker, 2000; Rohling *et al.*, 2003). An additional record
19
20 256 from the Barra Fan based on the planktonic foraminiferal assemblages in core VE56/-10/36
21
22 257 also shows a variation in SST around the time of GI-1d (Kroon *et al.*, 1997). The occurrence
23
24 258 of these brief periods of lower SST would favour the southerly penetration of icebergs calved
25
26 259 from the surviving North Atlantic ice sheets because of the fundamental control SST has on
27
28 260 the survival of icebergs in the ocean (Dowdeswell and Murray, 1990). Given the absence of
29
30 261 IRD at times of higher SST's when there was a continuing flux of icebergs from the same
31
32 262 potential sources, it is likely that it is SST which was the fundamental control on IRD
33
34 263 dispersal to the sub-polar North Atlantic during GI-1. The occurrence of a peak in IRD flux
35
36 264 associated with GI-1d is inferred to be the result of the attendant reduction in SST's associated
37
38 265 with this climatic oscillation.
39
40
41
42

43
44 266 SST's in the North Atlantic depend strongly on AMOC, with a weaker AMOC
45
46 267 associated with lower SST's at higher latitudes (Schmittner *et al.*, 2005; Barker *et al.*,
47
48 268 2009). Rerouting events have been identified that correspond to the abrupt climate
49
50 269 reversals of the last deglaciation (Clark *et al.*, 2001) and one such release of freshwater is
51
52 270 proposed as the cause of GI-1d and its concomitant cooling that is seen across the North
53
54 271 Atlantic (Rasmussen *et al.*, 2006; Thornalley *et al.*, 2010). This freshwater input, likely
55
56 272 caused an AMOC slowdown with an associated decrease in SST's, visible in the
57
58
59
60

1
2
3 273 palaeorecords and sufficient to allow icebergs (and IRD) to reach MD95-2007 and other ice
4
5 274 distal sites.
6
7

8 275 The LGIT was punctuated by periods of increased meltwater input from the decaying
9
10 276 ice sheets (Fairbanks, 1989; Hanebuth *et al.*, 2000; Bard *et al.*, 2010). These meltwater pulses
11
12 277 had various sources but their effects, both in terms of sea level rise and climate, were
13
14 278 widespread (Stanford *et al.*, 2006; Stanford *et al.*, 2010). The largest of the identified
15
16 279 meltwater pulses is MWP-1a, whose initial contributor is thought to be the Antarctic Ice Sheet
17
18 280 (AIS), where partial collapse released freshwater into the Southern Ocean (Clark *et al.*,
19
20 281 2002a). Resumption in NADW formation forced by a Southern injection of meltwater and
21
22 282 resulting in warming in the Northern Hemisphere (Weaver *et al.*, 2003) would explain the
23
24 283 Bølling warming that marks the end of the LGM and the start of GI-1 (Lowe *et al.*, 2008).
25
26 284 This warming would have favoured melting of the Northern Hemisphere ice sheets which
27
28 285 would have made a subsequent contribution to MWP-1a (Carlson *et al.*, 2012), in turn
29
30 286 diminishing the vigour of AMOC. This interaction produces a feedback between ice sheets
31
32 287 and climate (Clark *et al.*, 2001; McManus *et al.*, 2004; Meissner and Clark, 2006; Clarke *et*
33
34 288 *al.*, 2009; Thornalley *et al.*, 2010; He *et al.*, 2013). The evidence presented in this study
35
36 289 demonstrates a rapid alteration to the North Atlantic surface hydrography during the last
37
38 290 deglaciation, in agreement with this proposed feedback mechanism.
39
40
41
42
43
44
45

291

292 **5. Conclusions and Implications**

293 The co-registered, high-resolution IRD_{flux} and $\delta^{18}O_{foram}$ records from MD95-2007
48
49 294 provide evidence of an IRD peak during GI-1 that is coincident with a period of lower
50
51 295 $\delta^{18}O_{foram}$ values. The timing of this event is constrained using ^{14}C dates and tuning of the
52
53 296 record to NGRIP and is correlated with the short-lived cooling episode GI-1d (14,075-13,954
54
55 297 a b2k). Given our knowledge of the distribution of the pan-North Atlantic ice sheets and IRD
56
57
58
59
60

1
2
3 298 provenance fingerprinting using U-Pb dating of detrital minerals (Small *et al.*, 2013) it has
4
5 299 been established that the IRD peak in MD95-2007 reflects input of distally sourced material.
6
7 300 The absence of IRD in southerly (ice distal) cores at times when its flux at a northerly (ice
8
9 301 proximal) core was continuing suggests that IRD flux to the wider North Atlantic from the
10
11 302 surviving ice sheets is not the primary control. To explain this pattern of IRD occurrence it is
12
13 303 necessary to invoke a hydrographic control that prevents IRD deposition at ice distal sites
14
15 304 except during a defined cold interval, namely lowered SST.
16
17
18

19 305 The release of freshwater into the North Atlantic is proposed as the driving mechanism
20
21 306 of the short-lived and abrupt climate variations such as GI-1d. The effects of freshwater input
22
23 307 to the North Atlantic are primarily manifested through a slowdown of AMOC that reduces
24
25 308 SST's. A reduction in SST's favours the survival of icebergs and their wider dispersal. As
26
27 309 such we suggest that it is by this mechanism that IRD was deposited within these sub-polar
28
29 310 cores during GI-1d. The widespread effects of meltwater input to the North Atlantic during
30
31 311 the LGIT are clearly documented, but our evidence is some of the first that does not rely on
32
33 312 planktonic foraminiferal $\delta^{18}\text{O}$ alone.
34
35
36
37

38 313 Our conclusion that the GI-1 IRD peak within MD95-2007 contains distal material
39
40 314 (Small *et al.*, 2013) and that hydrographic conditions are important controls on sub-polar IRD
41
42 315 dispersal has far reaching implications. IRD has regularly been used to infer fine scale
43
44 316 behaviour of individual ice sheets. For example, IRD deposited during the last glacial cycle in
45
46 317 the sub-polar North Atlantic records sub-Milankovitch (millennial) scale climatic changes that
47
48 318 have been linked to the abrupt calving dynamics of marine ice-sheet margins (eg: Knutz *et al.*,
49
50 319 2001; Scourse *et al.*, 2009; Hibbert *et al.*, 2010). By combining geographically distinct IRD
51
52 320 records, information regarding IRD flux to the wider ocean, and IRD provenance studies it is
53
54 321 possible to demonstrate that hydrography may be an important additional control on IRD
55
56 322 occurrence. Our results highlight, particularly at the millennial and sub-millennial scale, that
57
58
59
60

1
2
3 323 IRD flux records may reflect a complex interplay between changes to oceanic conditions and
4
5 324 ice sheet calving dynamics.
6
7

8 325
9

10
11 326 **Acknowledgments**
12

13
14 327 This work was undertaken while DS was in receipt of a SAGES PhD studentship at the
15
16 328 University of St Andrews. We thank the captain and crew of the RV Marion Dufresne (MD
17
18 329 101) for core collection. We thank the captain and crew of the RV Marion Dufresne (MD 101)
19
20 330 and L. Labeyrie, in particular. R. Sørås and C. Murray provided technical assistance. Support
21
22 331 for this research to WENA was provided from the NERC RAPID programme, NERC RCL,
23
24 332 the Universities of St Andrews and Bergen and the WHOI-Mary Sears Fund. We would like
25
26 333 to thank two anonymous reviewers for constructive comments that have improved the
27
28 334 manuscript.
29
30

31
32 335
33
34

35 336
36
37
38
39
40
41
42
43
44
45
46
47
48
49
50
51
52
53
54
55
56
57
58
59
60

1
2
3 337 **References**
4

5 338

6
7 339 Alley RB, Marotzke J, Nordhaus WD, Overpeck JT, Peteet DM, Pielke Jr. RA, Pierrehumbert
8 340 RT, Rhines PB, Stocker TF, Talley LD, Wallace JM. 2003, Abrupt Climate Change, *Science*,
9 341 **299**: 2005-2010.

11 342

12
13 343 Andrews JT. 2000, Icebergs and iceberg rafted detritus (IRD) in the North Atlantic: faacts and
14 344 assumptions. *Oceanography*, **13**: 100-108.

16 345

17
18 346 Austin WEN. 1991, Late Quaternary benthonic foraminiferal startigraphy of the western UK
19 347 continental shelf, *Unpublished PhD Thesis*, University of Wales.

21 348

22
23 349 Austin WEN, Kroon D. 1996, Late glacial sedimentology, foraminifera and stable isotope
24 350 stratigraphy of the Hebridean Continental Shelf, northwest Scotland, *Geological Society*,
25 351 *London, Special Publications*, **111**: 187-213.

27 352

28
29 353 Austin WEN, Kroon D. 2001, Deep sea ventilation of the northeastern Atlantic during the last
30 354 15,000 years, *Global and Planetary Change*, **30**: 13-31.

32 355

33
34 356 Austin WEN, Hibbert FD. 2012, Tracing time in the ocean: a brief review of chronological
35 357 constraints (60-18 ka) on North Atlantic marine event-based stratigraphies, *Quaternary*
36 358 *Science Reviews*, **36**: 28-37.

38 359

39
40 360 Austin WEN, Bard E, Hunt JB, Kroon D, Peacock, JD. 1995, The ¹⁴C age of the Icelandic
41 361 Vedde Ash: Implications for Younger Dryas marine reservoir age corrections., *Radiocarbon*,
42 362 **37**: 53-62.

44 363

45
46 364 Austin WEN, Telford RJ, Ninnemann US, Brown L, Wilson LJ, Small DP, Bryant CL. 2011,
47 365 North Atlantic reservoir ages linked to high Younger Dryas atmospheric radiocarbon
48 366 concentrations, *Global and Planetary Change*, **79**: 226-233.

50 367

51
52 368 Ballantyne CKB, Stone JO. 2012, Did large ice caps persist on low ground in north-west
53 369 Scotland during the Lateglacial Interstade, *Journal of Quaternary Science*, **27**: 297-306.

55 369

56
57
58
59
60

- 1
2
3 370
4
5 371 Bard E, Hamelin B, Delanghe-Sabatier D. 2010, Deglacial Meltwater Pulse 1B and Younger
6 372 Dryas Sea Levels Revisited with Boreholes at Tahiti, *Science*, **327**: 1235-1237.
7
8 373
9
10 374 Barker S, Diz P, Vautravers MJ, Pike J, Knorr G, Hall IR, Broecker WS. 2009,
11 375 Interhemispheric Atlantic seesaw response during the last deglaciation, *Nature*, **457**: 1097-
12 376 1102.
13
14 377
15
16 378 Bronk Ramsey, C. 2009. Bayesian analysis of radiocarbon dates, *Radiocarbon*, **51** 337-360.
17 379
18
19 380 Bjorck S, Kromer B, Johnsen S, Bennike O, Hammarlund D, Lemdahl G, Possnert G,
20 381 Rasmussen TL, Wohlfarth B, Hammer CU, Spurk M. 1996, Synchronized terrestrial-
21 382 atmospheric deglacial records around the North Atlantic, *Science*, **274**: 1155-1160.
22 383
23
24 384 Bond G, Broecker WS, Johnsen S, McManus J, Labeyrie L, Jouzel J, Bonani, G. 1993,
25 385 Correlations between climate records from North Atlantic sediments and Greenland ice,
26 386 *Nature*, **365**: 143-147.
27
28 387
29
30 388 Bradwell T, Fabel D, Stoker M, Mathers H, McHargue L, Howe J. 2008, Ice caps existed
31 389 throughout the Lateglacial Interstadial in northern Scotland, *Journal of Quaternary Science*,
32 390 **23**: 401-407.
33 391
34
35 392 Broecker WS. 1994, Massive iceberg discharges as triggers for global climate change, *Nature*,
36 393 **372**: 421-424.
37 394
38
39 395 Broecker WS. 2000, Abrupt climate change: causal constraints provided by the paleoclimate
40 396 record, *Earth-Science Reviews*, **51**: 137-154.
41
42 397
43
44 398 Carlson AE, Ullman DJ, Anslow FS, He F, Clark PU, Liu Z, Otto-Bliesner BL. 2012,
45 399 Modeling the surface mass-balance response of the Laurentide Ice Sheet to Bølling warming
46 400 and its contribution to Meltwater Pulse 1A, *Earth and Planetary Science* **315-316**: 24-29.
47 401
48
49 402 Clark PU, Pisias NG, Stocker TF, Weaver AJ. 2002, The role of the thermohaline circulation
50 403 in abrupt climate change, *Nature*, **415**: 863-869.
51
52
53
54
55
56
57
58
59
60

1
2
3 404

4 405 Clark PU, Marshall SJ, Clarke GKC, Hostetler SW, Licciardi JM, Teller JT. 2001, Freshwater
5 406 Forcing of Abrupt Climate Change During the Last Glaciation, *Science*, **293**: 283-287.

6
7
8 407

9 408 Clarke GKC, Bush ABG, Bush JWM. 2009, Freshwater Discharge, Sediment Transport, and
10 409 Modeled Climate Impacts of the Final Drainage of Glacial Lake Agassiz, *Journal of Climate*,
11 410 **22**: 2161-2180.

12
13
14 411

15 412 Davies HC, Dobson MR, Whittington RJ. 1984, A revised seismic stratigraphy for Quaternary
16 413 deposits on the inner continental shelf west of Scotland between 55°30'N and 57°30'N,
17 414 *Boreas*, **13**: 49-66.

18
19
20 415

21 416 Dowdeswell JA, Murray T. 1990, Modelling rates of sedimentation from icebergs, *Geological*
22 417 *Society, London, Special Publications*, **53**: 121-137.

23
24
25 418

26 419 Elliot M, Labeyrie L, Duplessy, JC 2002, Changes in North Atlantic deep-water formation
27 420 associated with the Dansgaard-Oeschger temperature oscillations (60-10 ka), *Quaternary*
28 421 *Science Reviews*, **21**: 1153-1165.

29
30
31 422

32 423 Elliot M, Labeyrie L, Dokken T, Manthe S. 2001, Coherent patterns of ice-rafted debris
33 424 deposits in the Nordic regions during the last glacial (10-60 ka), *Earth and Planetary Science*
34 425 *Letters*, **194**: 151-163.

35
36
37 426

38 427 Fairbanks RG. 1989, A 175,000-year glacio-eustatic sea level record: influence of glacial
39 428 melting rates on the Younger Dryas event and deep-ocean circulation., *Nature*, **342**: 637-642.

40
41
42 429

43 430 Grootes PM, Stuiver M. 1997, Oxygen 18/16 variability in Greenland snow and ice with 10-
44 431 3-to 105-year time resolution. *Journal of Geophysical Research* **102**: 26455-26470.

45
46
47 432

48 433 Hanebuth T, Statterger K, Grootes PM. 2000, Rapid Flooding of the Sunda Shelf: A Late-
49 434 Glacial Sea-Level Record, *Science*, **288**: 1033-1035.

50
51
52 43553
54
55
56
57
58
59
60

- 1
2
3 436 He F, Clark PU, Carlson AE., Liu Z, Otto-Bliesner BL, Kutzbach JL. 2013, Northern
4 437 Hemisphere forcing of Southern Hemisphere climate during the last deglaciation, *Nature*, **494**:
5 438 81-85.
6
7 439
8
9 440 Heinrich H. 1988, Origin and consequences of cyclic ice rafting in the Northeast Atlantic
10 441 Ocean during the past 130,000 years, *Quaternary Research*, **29**: 142-152.
11
12 442
13
14 443 Hemming SR. 2004, Heinrich events: Massive late Pleistocene detritus layers of the North
15 444 Atlantic and their global climate imprint, *Reviews in Geophysics*, **42**: RG1005.
16
17 445
18
19 446 Hendy IL, Cosma T. 2008, Vulnerability of the Cordilleran Ice Sheet to iceberg calving during
20 447 late Quaternary rapid climate change events, *Paleoceanography*, **23**: PA2101.
21
22 448
23
24 449 Hibbert FD, Austin WEN, Leng MJ, Gatliff RW. 2010, British Ice Sheet dynamics inferred
25 450 from North Atlantic ice-rafted debris records spanning the last 175 000 years, *Journal of*
26 451 *Quaternary Science*, **25**: 461-482.
27
28 452
29
30 453 Knutz PC, Austin WEN, Jones EJW. 2001, Millennial-scale depositional cycles related to
31 454 British Ice Sheet variability and North Atlantic paleocirculation since 45 kyr BP, Barra Fan,
32 455 UK margin, *Paleoceanography*, **16**: 53-64.
33
34 456
35
36 457 Knutz PC, Zahn R, Hall IR. 2007, Centennial-scale variability of the British Ice Sheet:
37 458 Implications for climate forcing and Atlantic meridional overturning circulation during the last
38 459 deglaciation, *Paleoceanography*, **22**: PA1207.
39
40 460
41
42 461 Kroon D, Austin WEN, Chapman MR, Ganssen GM. 1997, Deglacial Surface Circulation
43 462 Changes in the Northeastern Atlantic: Temperature and Salinity Records off NW Scotland on
44 463 a Century Scale, *Paleoceanography*, **12**: 755-763.
45
46 464
47
48 465 LeGrande AN, Schmidt GA, Shindell DT, Field CV, Miller RL, Koch DM, Faluvegi G,
49 466 Hoffmann G. 2006, Consistent simulations of multiple proxy responses to an abrupt climate
50 467 change event, *Proceedings of the National Academy of Sciences of the United States of*
51 468 *America*, **103**: 837-842.
52
53 469
54
55
56
57
58
59
60

- 1
2
3 470 Liu Z, Otto-Bliesner BL, He F, Brady EC, Thomas R, Clark PU, Carlson AE, Lynch-Stieglitz
4 471 J, Curry W, Brook E, Erickson D, Jacob R, Kutzbach J, Cheng J. 2009, Transient Simulation
5 472 of Last Deglaciation with a New Mechanism for Bølling-Allerød Warming, *Science*, **325**: 310-
6 473 314.
7
8 474
9
10 475
11 475 Lowe JJ , Rasmussen SO, Bjorck S, Hoek WZ, Steffensen JP, Walker MJC, Yu ZC. 2008,
12 476 Synchronisation of palaeoenvironmental events in the North Atlantic region during the Last
13 477 Termination: a revised protocol recommended by the INTIMATE group, *Quaternary Science*
14 478 *Reviews*, **27**: 6-17.
15
16 479
17
18 480
19 480 Marshall SJ, Koutnik MR. 2006, Ice sheet action versus reaction: Distinguishing between
20 481 Heinrich events and Dansgaard-Oeschger cycles in the North Atlantic, *Paleoceanography*, **21**:
21 482 PA2021.
22
23 483
24
25 484
26 484 McCabe AM, Clark PU. 1998, Ice-sheet variability around the North Atlantic Ocean during
27 485 the last deglaciation, *Nature*, **392**: 373-377.
28
29 486
30
31 487
32 487 McManus JF, Bond, GC, Broecker WS, Johnsen S, Labeyrie L, Higgins S. 1994. High-
33 488 resolution climate records from the North Atlantic during the last interglacial. *Nature*, **371**:
34 489 326-329.
35
36 490
37
38 491
39 491 McManus JF, Francois R, Gherardi JM, Keigwin LD, Brown-Leger S. 2004, Collapse and
40 492 rapid resumption of Atlantic meridional circulation linked to deglacial climate changes,
41 493 *Nature*, **428**: 834-837.
42
43 494
44
45 495
46 495 Meissner KJ, Clark PU. 2006, Impact of floods versus routing events on the thermohaline
47 496 circulation, *Geophysical Research Letters*, **33**: L15704.
48
49 497
50 498
51 498 Naafs BDA, Hefter J, Ferretti P, Stein R, Haug GH. 2011, Sea surface temperatures did not
52 499 control the first occurrence of Hudson Strait Heinrich Events during MIS 16,
53 500 *Paleoceanography*, **26**: PA4201.
54
55 501
56
57
58
59
60

- 1
2
3 502 Peacock JD, Austin WEN, Selby I, Graham DK, Harland R, Wilkinson IP. 1992, Late
4 503 Devensian and Flandrian palaeoenvironmental changes on the Scottish continental shelf west
5 504 of the Outer Hebrides, *Journal of Quaternary Science*, **7**: 145-161.
6
7
8 505
9
10 506 Peck VL, Hall IR, Zahn R, Grousset F, Hemming SR, Scourse JD. 2007, The relationship of
11 507 Heinrich events and their European precursors over the past 60 ka BP: a multi-proxy ice-rafted
12 508 debris provenance study in the North East Atlantic, *Quaternary Science Reviews*, **26**: 862-875.
13
14 509
15
16 510 Peters C, Austin WEN, Walden J, Hibbert FD. 2010, Magnetic characterisation and
17 511 correlation of a Younger Dryas tephra in North Atlantic marine sediments, *Journal of*
18 512 *Quaternary Science*, **25**: 339-347.
19
20
21 513
22
23 514 Rahmstorf S. 2002, Ocean circulation and climate during the past 120,000 years, *Nature*, **419**:
24 515 207-214.
25
26 516
27
28 517 Rasmussen SO, Andersen KK, Svensson AM, Steffensen JP, Vinther BM, Clausen HB,
29 518 Siggard-Andersen M-L, Johnsen SJ, Larsen LB, Dahl-Jensen D, Bigler M, Röthlisberger R,
30 519 Fischer H, Goto-Azuma K, Hansson ME, Ruth U. 2006, A new Greenland ice core
31 520 chronology for the last glacial termination, *Journal of Geophysical Research*, **111**: D06102.
32
33 521
34
35 522 Reimer PJ, Baillie MGL, Bard E, Bayliss A, Beck JW, Blackwell PG, Bronk Ramsey C, Buck
36 523 CE, Burr GS, Edwards RL, Friedrich M, Grootes PM, Guilderson TP, Hajdas I, Heaton TJ,
37 524 Hogg AG, Hughen KA, Kaiser KF, Kromer B, McCormac FG, Manning SW, Reimer RW,
38 525 Richards DA, Southon JR, Talamo S, Turney CSM, van der Plicht J, Weyhenmeyer CE. 2009,
39 526 INTCAL09 and MARINE09 radiocarbon age calibration curves, 0–50,000 years cal BP,
40 527 *Radiocarbon*, **51**: 1111-1150.
41 528
42
43 529 Rohling ER, Mayewski PM, Challenor PC. 2003, On the timing and mechanism of millennial-
44 530 scale climate variability during the last glacial cycle, *Climate Dynamics*, **20**: 257-267.
45
46 531
47
48 532 Ruddiman WF. 1977. Late Quaternary deposition of ice-rafted sand in the subpolar North
49 533 Atlantic (lat 40 to 65 N). *Geological Society of America Bulletin*, **88**: 1813-1827.
50
51 534
52
53
54
55
56
57
58
59
60

1
2
3 535 Ruddiman WF, McIntyre A. 1981. The North Atlantic Ocean during the last deglaciation.
4 536 *Palaeogeography, Palaeoclimatology, Palaeoecology*, **35**: 145-214.

5
6 537

7
8 538 Schmittner A, Latif M, Schneider B. 2005, Model projections of the North Atlantic
9 thermohaline circulation for the 21st century assessed by observations, *Geophysical Research*
10 539 *Letters*, **32**: L23710.

11
12
13 541

14 542 Scourse JD, Haapaniemi AI, Colmenero-Hidalgo E, Peck VL, Hall IR, Austin WEN, Knutz
15 PC, Zahn R. 2009, Growth, dynamics and deglaciation of the last British-Irish ice sheet: the
16 543 deep-sea ice-rafted detritus record, *Quaternary Science Reviews*, **28**: 3066-3084.

17
18 544
19
20 545

21 546 Severinghaus JP, Brook EJ. 1999, Abrupt Climate Change at the End of the Last Glacial
22 547 Period Inferred from Trapped Air in Polar Ice, *Science*, **286**: 930-934.

23
24 548

25
26 549 Simpson MJR, Milne GA, Huybrechts P, Long AJ. 2009, Calibrating a glaciological model of
27 the Greenland ice sheet from the Last Glacial Maximum to present-day using field
28 550 observations of relative sea level and ice extent, *Quaternary Science Reviews*, **28**: 1631-1657.

29
30 551
31 552

32
33 553 Small D, Parrish RR, Austin WEN, Cawood PA, Rinterknecht V. 2013, Provenance of North
34 554 Atlantic ice-rafted debris during the last deglaciation- A new application of U-Pb rutile and
35 zircon geochronology, *Geology*, **45**: 155-158.

36
37 555
38 556

39 557 Stanford JD, Rohling EJ, Hunter SE, Roberts AP, Rasmussen SO, Bard E, McManus J,
40 558 Fairbanks RG. 2006, Timing of meltwater pulse 1a and climate responses to meltwater
41 559 injections, *Paleoceanography*, **21**: PA4103.

42
43
44 560

45
46 561 Stanford JD, Hemingway R, Rohling EJ, Challenor PG, Medina-Elizalde M, Lester AJ. 2010,
47 562 Sea-level probability for the last deglaciation: A statistical analysis of far-field records, *Global*
48 563 *and Planetary Change*, **79**: 193-203.

49
50 564

51
52
53 565 Stanford JD, Rohling EJ, Bacon S, Roberts AP, Grousset FE, Bolshaw M. 2011, A new
54 566 concept for the paleoceanographic evolution of Heinrich event 1 in the North Atlantic,
55 567 *Quaternary Science Reviews*, **30**: 1047-1066.

56
57
58 568

59
60

- 1
2
3 569 Steffensen JP, et al. 2008, High-Resolution Greenland Ice Core Data Show Abrupt Climate
4 570 Change Happens in Few Years, *Science*, **321**: 680-684.
5
6 571
7
8 572 Stoker M, Hitchen K, Graham CC. 1993, *United Kingdom Offshore Report: the Geology of*
9 *the Hebrides and West Shetland Shelves, and Adjacent Deep-water Areas.*, HMSO for the
10 573 British Geological Survey, London.
11 574
12
13 575
14 576 Stuiver M, Reimer, PJ. 1993, Extended ^{14}C database and revised CALIB 3.0 ^{14}C age
15 577 calibration program, *Radiocarbon*, **35**: 215-230.
16
17 578
18
19 579 Stuiver M, Reimer PJ, Bard E, Beck JW, Burr GS, Hughen KA, Kromer B, McCormac FG,
20 580 van der Plicht J, Spurk M. 1998, INTCAL98 radiocarbon age calibration, 24,000-0 cal BP,
21 581 *Radiocarbon*, **40**: 1041-1083.
22
23 582
24
25 583 Thornalley DJR, McCave IN, Elderfield H. 2010, Freshwater input and abrupt deglacial
26 584 climate change in the North Atlantic, *Paleoceanography*, **25**: PA1201.
27
28 585
29
30 586 Vidal L, Labeyrie L, Cortijo E, Arnold M, Duplessy JC, Michel E, Becque S, van Weering
31 587 TCE. 1997, Evidence for changes in the North Atlantic Deep Water linked to meltwater surges
32 588 during the Heinrich events, *Earth and Planetary Science Letters*, **146**: 13-27.
33
34 589
35
36 590 Waelbroeck C, Duplessy JC, Michel E, Labeyrie L, Paillard D, Duprat J. 2001, The timing of
37 591 the last deglaciation in North Atlantic climate records, *Nature*, **412**: 724-727.
38
39 592
40
41 593 Weaver AJ, Saenko OA, Clark PU, Mitrovica JX. 2003, Meltwater Pulse 1A from Antarctica
42 594 as a Trigger of the Bølling-Allerød Warm Interval, *Science*, **299**: 1709-1713.
43
44 595
45
46 596 Wilson LJ. 2004, Late Quaternary Stratigraphies from the Hebridean Continental Shelf and
47 597 Margin, North West Scotland, United Kingdom., *Unpublished PhD Thesis*, University of St
48 598 Andrews.
49
50 599
51
52 600 Wilson LJ, Austin WEN, Jansen E. 2002, The last British Ice Sheet: growth, maximum extent
53 601 and deglaciation, *Polar Research*, **21**: 243-250.
54
55
56
57
58
59
60

1
2
3 6024
5 603 **Figure Caption**6
7 6048
9 605 Figure 1. Map of the North Atlantic showing the location of MD95-2007 (red star) and other
10 606 cores mentioned in the text. Also shown is the IRD belt of Ruddiman, (1977) and the
11 607 approximate location of the polar front (dashed red line) at various times in the past after
12 608 McManus *et al.*, (1994).
13
14
15

16 609

17
18
19 610 Figure 2. Final age model for MD95-2007. Tuning of the MD95-2007 benthic $\delta^{18}\text{O}_{\text{foram}}$
20 611 record (Austin *et al.*, 2011) to the NGRIP $\delta^{18}\text{O}$ record on the GICC05 timescale (Rasmussen
21 612 *et al.*, 2006). a) MD95-2007 benthic $\delta^{18}\text{O}$ against core depth; b) NGRIP $\delta^{18}\text{O}$; c) MD95-2007
22 613 benthic $\delta^{18}\text{O}$ tuned using basal AMS ^{14}C date corrected for $\Delta R = 300$. The solid lines show
23 614 the tie points based on major climate transitions visible in both records, the dashed line
24 615 indicates the basal radiocarbon age. Black dots on top axis are available ^{14}C dates. The
25 616 Vedde Ash isochron is labelled.
26
27
28
29
3031
32 61733
34 618 Figure 3. MD95-2007 $\delta^{18}\text{O}_{\text{foram}}$ plotted using 3 ‘preliminary’ age models constrained by the
35 619 available AMS ^{14}C dates (Table 1) calibrated using OxCal v4.1 and MARINE09 (Bronk
36 620 Ramsey, 2009; Reimer *et al.*, 2009) and three different values for ΔR ; 0, 300 and 700. The
37 621 tuned age model is shown for comparison.
38
39
40
41

42 622

43
44 623 Figure 4. MD95-2007 IRD_{flux} record plotted against $\delta^{18}\text{O}_{\text{foram}}$ record using the tuned age
45 624 model (Figure 2). The stratigraphic divisions are as recommended by INTIMATE (Lowe *et*
46 625 *al.*, 2008).
47
48
49

50 626

51
52
53 627 Figure 5. Composite stratigraphic plot of the IRD records discussed in the text plotted on their
54 628 original timescales. The tuned proxies from MD95-2007 (this study; Austin *et al.*, 2011),
55 629 DAPC-2 (Knutz *et al.*, 2007) and RAPid-15-4P (Thornalley *et al.*, 2010) are shown alongside
56 630 the IRD records. The NGRIP $\delta^{18}\text{O}$ record (Rasmussen *et al.*, 2006) is shown alongside the
57
58
59
60

1
2
3 631 IRD record from TTR-451 (Stanford *et al.*, 2011). The age offset between DAPC-2 and the
4 632 other records is the result of this record being tied to GISP2 $\delta^{18}\text{O}$ (Groots and Stuiver, 1997);
5
6 633 the other records were tied to NGRIP $\delta^{18}\text{O}$ on the GICC05 timescale (Rasmussen *et al.*, 2006).
7
8

9 634
10
11
12
13
14
15
16
17
18
19
20
21
22
23
24
25
26
27
28
29
30
31
32
33
34
35
36
37
38
39
40
41
42
43
44
45
46
47
48
49
50
51
52
53
54
55
56
57
58
59
60

635

Table 1. ^{14}C Ages from MD95-2007

Sample	Core depth (cm)	Radiocarbon age (^{14}C a BP $\pm 1\text{sigma}$)	Calibrated Age (cal a BP)			Original age*
			$\Delta\text{R}=0$	$\Delta\text{R}=300$	$\Delta\text{R}=700$	
AA-41753	21	2279 \pm 36	2285 \pm 62	1537 \pm 56	1140 \pm 51	1879
AA-41754	121	10664 \pm 65	12601 \pm 61	11394 \pm 143	10926 \pm 121	11825**
AA-41762	375.5	11353 \pm 62	13231 \pm 65	12583 \pm 81	11987 \pm 137	12907
AA-41755	396.5	11299 \pm 66	13195 \pm 72	12512 \pm 88	11873 \pm 158	12890
AAR-2602	425	11500 \pm 90	13355 \pm 97	12689 \pm 96	12249 \pm 164	13000
AA-41763	442.5	11296 \pm 77	13192 \pm 85	12494 \pm 98	11861 \pm 183	12889
AA-41756	556.5	11471 \pm 62	13331 \pm 67	12657 \pm 67	12202 \pm 128	12990
AA-41757	741.5	12353 \pm 74	14396 \pm 247	13502 \pm 101	13152 \pm 98	13832
AAR-2603	826	12630 \pm 100	14880 \pm 275	13777 \pm 127	13379 \pm 111	14109
AAR-2604	974.5	12790 \pm 120	15235 \pm 352	13949 \pm 194	13545 \pm 129	14289
AA-41758	1008.5	12789 \pm 88	15211 \pm 271	13926 \pm 121	13542 \pm 108	14289
AA-41759	1345.5	12953 \pm 74	15526 \pm 318	14133 \pm 229	13695 \pm 105	14721**
AAR-2605	1663	13810 \pm 170	16925 \pm 198	15890 \pm 416	15028 \pm 457	15995
AA-41760	1674	13020 \pm 110	15721 \pm 366	14356 \pm 280	13765 \pm 137	14739**
AAR-2606	1815.5	14250 \pm 150	17346 \pm 222	16664 \pm 279	15958 \pm 402	16502
AA-41761	1821	13950 \pm 130	17029 \pm 170	16152 \pm 385	15384 \pm 374	16157

Ages calibrated using OxCal v4.1, MARINE09. $\Delta\text{R} = 0, 300$ & 700 (Bronk Ramsey, 2009; Reimer et al., 2009)

*Ages from Wilson (2004) calibrated using Calib4_2 $\Delta\text{R} = 0$, uncertainties not reported.

** Average of 3 ages from shell fragments

636

637

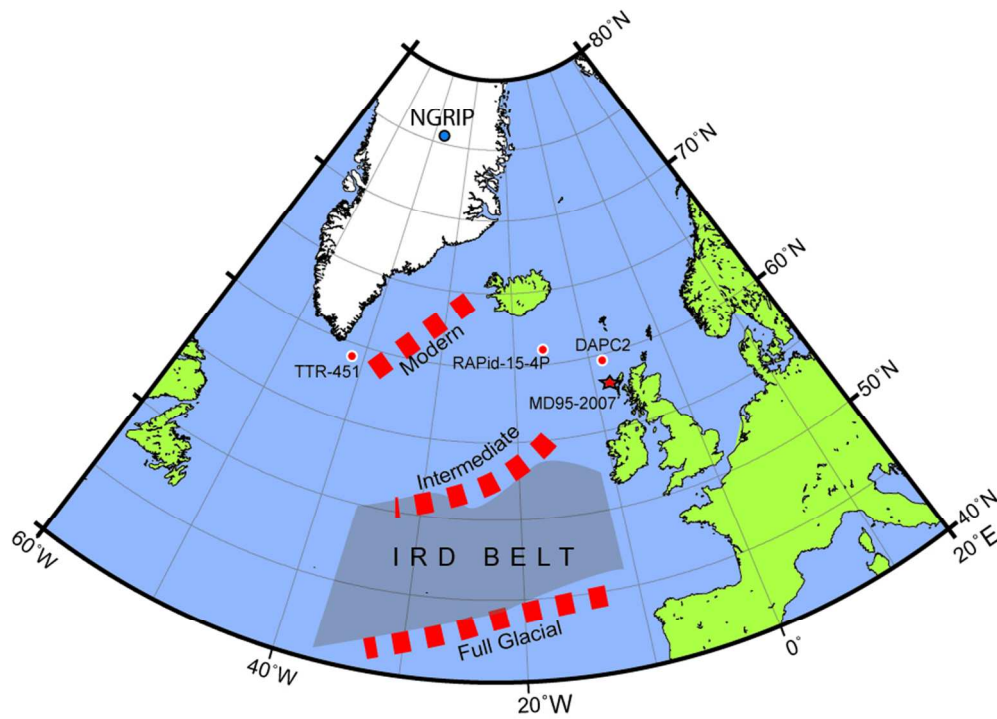
Table 2. Tie points used in construction of tuned age model.

Tie Point	Core depth (cm)	Age assigned (a b2k)	Reference
End of GS-1	101	11703	Lowe et al. 2008
Vedde Ash	281	12171	Rasmussen et al. 2006
Start of GS-1	521	12896	Lowe et al. 2008
End of GI-1d	941	13954	Lowe et al. 2008
Start of GI-1d	1016	14075	Lowe et al. 2008

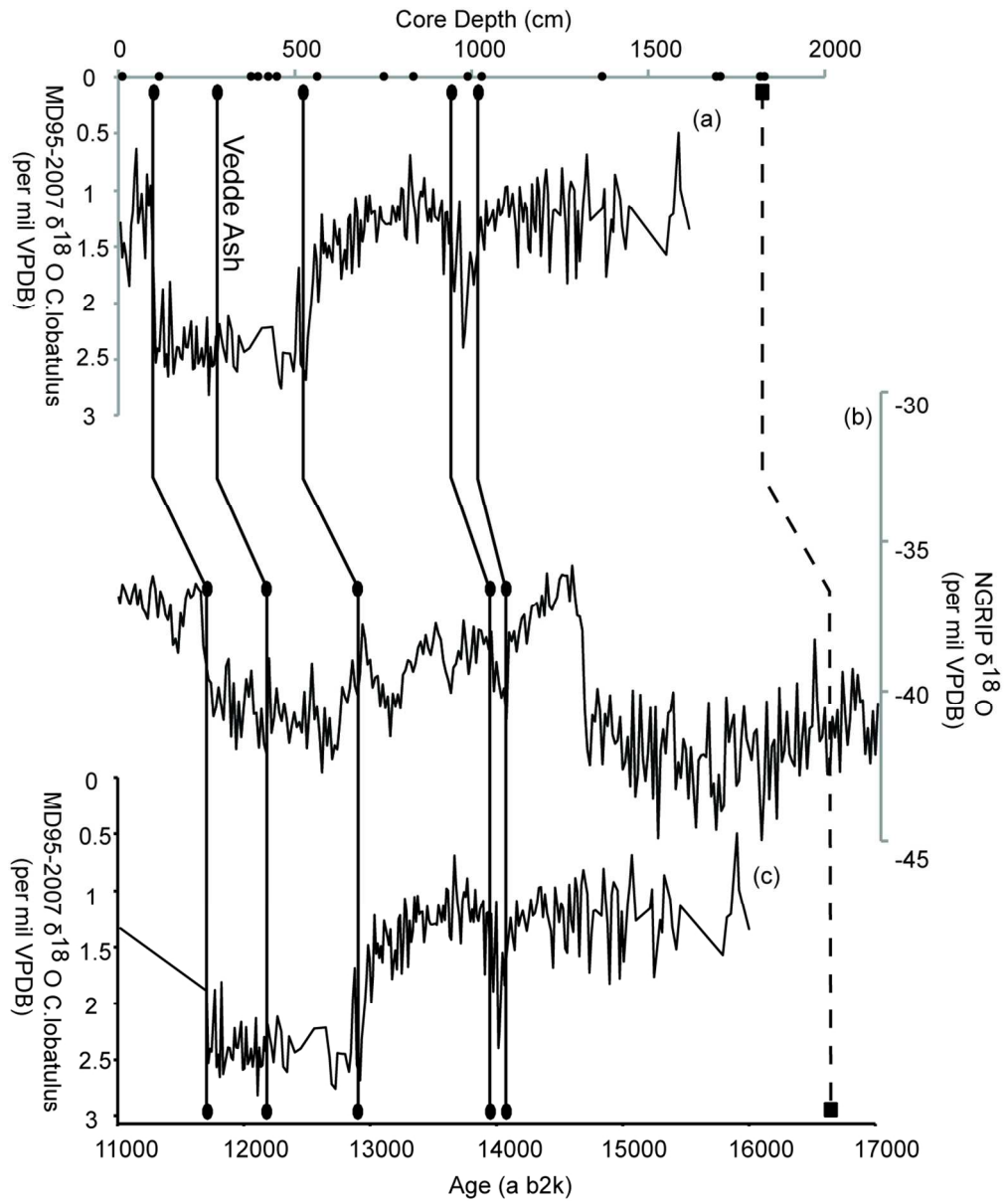
638

639

1
2
3
4
5
6
7
8
9
10
11
12
13
14
15
16
17
18
19
20
21
22
23
24
25
26
27
28
29
30
31
32
33
34
35
36
37
38
39
40
41
42
43
44
45
46
47
48
49
50
51
52
53
54
55
56
57
58
59
60

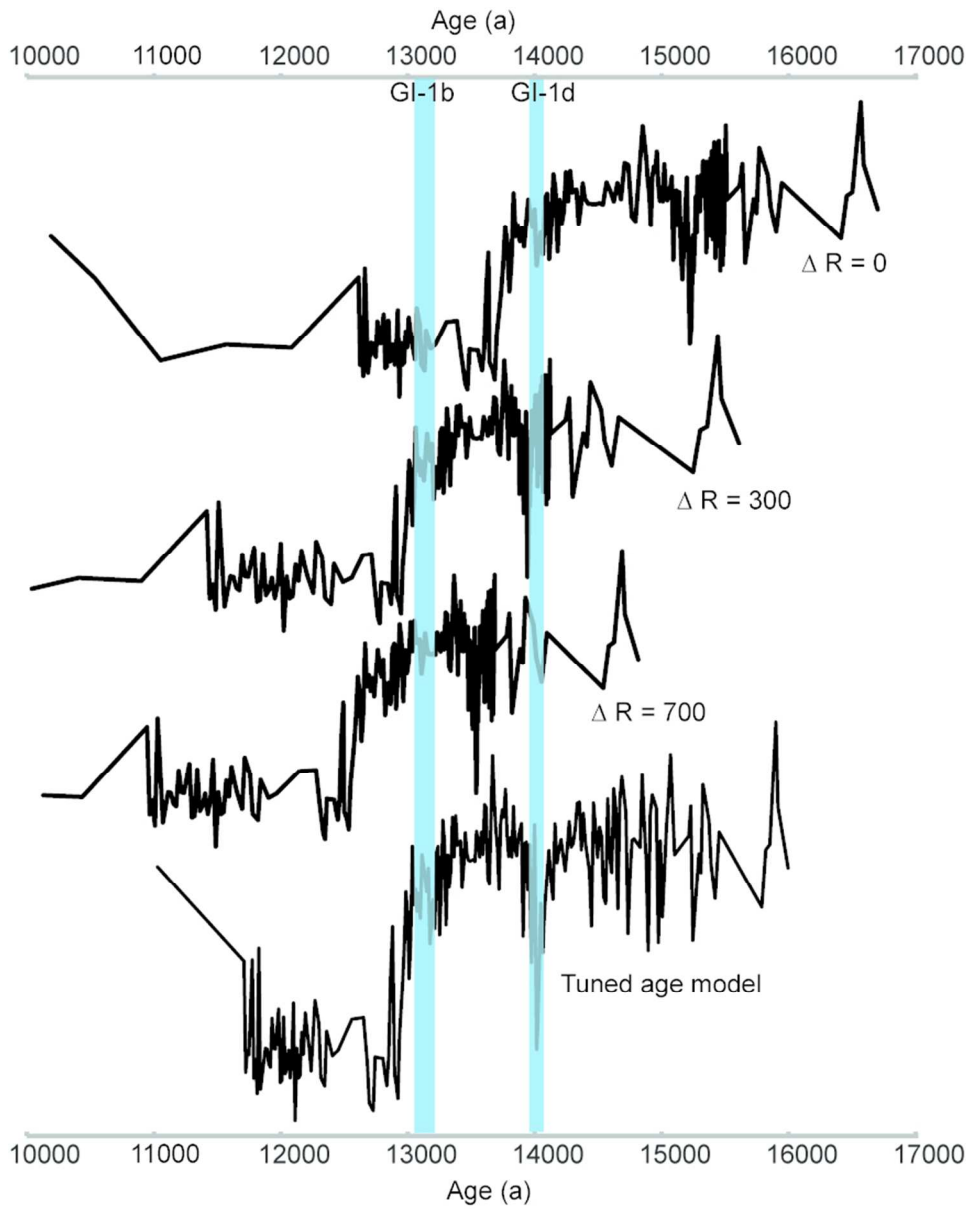


83x60mm (300 x 300 DPI)

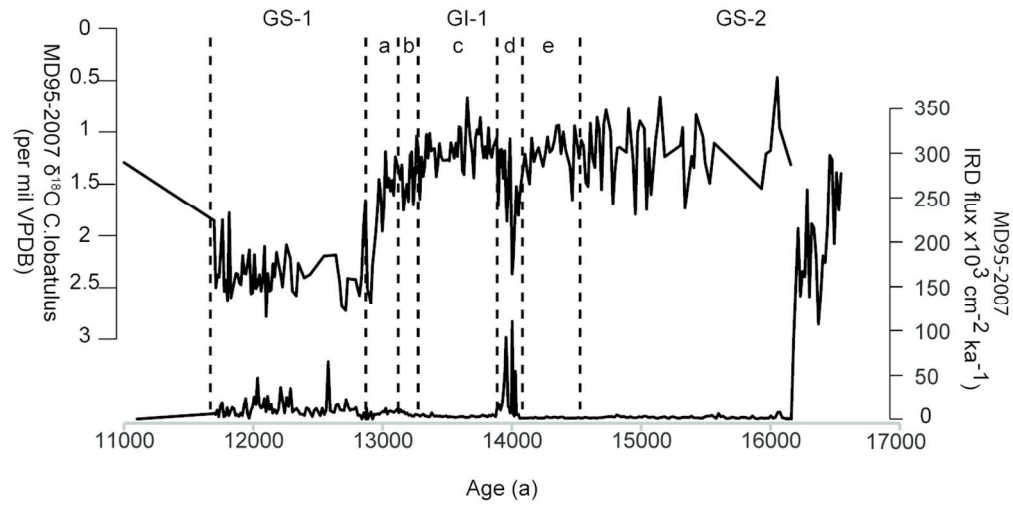


117x140mm (300 x 300 DPI)

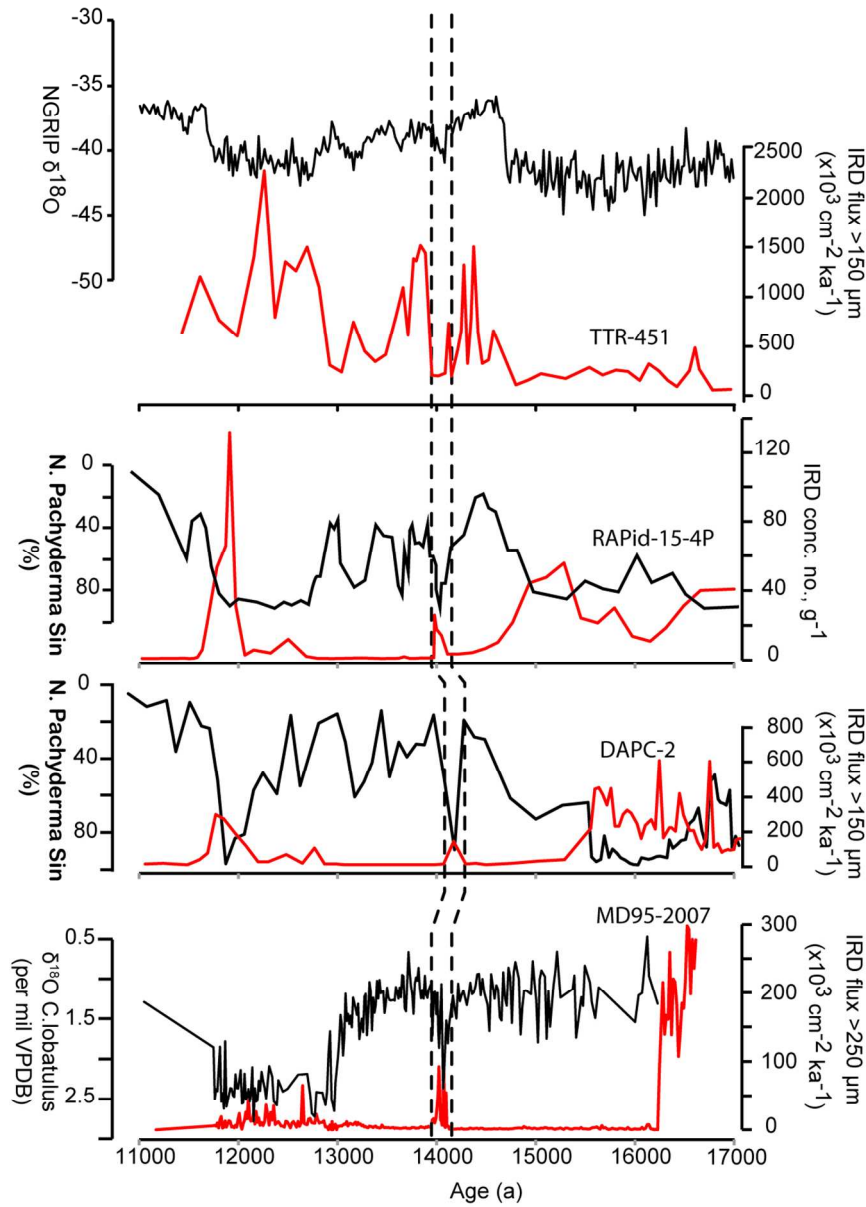
1
2
3
4
5
6
7
8
9
10
11
12
13
14
15
16
17
18
19
20
21
22
23
24
25
26
27
28
29
30
31
32
33
34
35
36
37
38
39
40
41
42
43
44
45
46
47
48
49
50
51
52
53
54
55
56
57
58
59
60



73x92mm (300 x 300 DPI)



116x57mm (300 x 300 DPI)



117x142mm (300 x 300 DPI)